Journal of Medicinal Chemistry Article

J. Med. Chem. **2009,** *52,* 7993–8001 **7993**
DOI: 10.1021/jm901023f

In Vitro and In Vivo Isotope Effects with Hepatitis C Protease Inhibitors: Enhanced Plasma Exposure of Deuterated Telaprevir versus Telaprevir in Rats

François Maltais, Young Chun Jung, Minzhang Chen, Jerry Tanoury, Robert B. Perni,[†] Nagraj Mani, Leena Laitinen, Hui Huang, Shengkai Liao, Hongying Gao,[‡] Hong Tsao, Eric Block, Chien Ma, Rebecca S. Shawgo, Christopher Town, Christopher L. Brummel, David Howe, S. Pazhanisamy, Scott Raybuck, Mark Namchuk, and Youssef L. Bennani*

Vertex Pharmaceuticals Incorporated, 130 Waverly Street, Cambridge, Massachusetts 02139. [†]*Sirtris, a GlaxoSmithKline company, 200 Technology Square, Cambridge, MA 02139.* [‡]*Pfizer Inc., 558 Eastern Point Rd, Groton, CT 06340-5196.*

Received July 10, 2009

Telaprevir **2** (VX-950), an inhibitor of the hepatitis C virus (HCV[a]) NS3-4A protease, is in phase 3 clinical trials. One of the major metabolites of **2** is its P1-(*R*)-diastereoisomer, **3** (VRT-394), containing an inversion at the chiral center next to the α-ketoamide on exchange of a proton with solvent. Compound **3** is approximately 30-fold less active against HCV protease. In an attempt to suppress the epimerization of **2** without losing activity against the HCV protease, the proton at that chiral site was replaced with deuterium (d). The compound **1** (d-telaprevir) is as efficacious as **2** in in vitro inhibition of protease activity and viral replication (replicon) assays. The kinetics of in vitro stability of **1** and **2** in buffered pH solutions and plasma samples, including human plasma, suggest that **1** is significantly more stable than **2**. Oral administration (10 mg/kg) in rats resulted in a ∼13% increase of AUC for **1**.

Introduction

Hepatitis C viral infection (HCV[a]) is a serious health crisis affecting over 180 million people worldwide.[1] The current approved therapy for chronic HCV is a combination of weekly injection of PEG-IFN-α with a twice-a-day oral administration of ribavirin.[2,3] Development of new therapies for hepatitis C is focusing on STAT-C compounds to directly block the viral life cycle. Most new compounds target the HCV NS5B polymerase or the NS3-4A protease,[4] an enzyme needed for the release of nonstructural proteins from the initially translated HCV polypeptide. Several polymerase and NS3-4A protease inhibitors have been advanced to clinical testing with varying degrees of success.[5−16] The HCV polymerase has multiple binding pockets and lends itself to inhibition by competitive inhibitors (NIs) and allosteric inhibitors (NNIs). Clinical trials of NS5B inhibitors are numerous; many failed after advancing to phase II trials due to adverse effects or viral rebound due to resistant strains. At present, Abbott (NNI), Anadys (NNI), and GSK (NNI) are in phase I; Gilead (NNI), Pfizer (NNI), and Pharmasset/Roche (NI) have advanced to phase II clinical trials.[5−8] The active site of HCV protease is shallow requiring multiple interactions from the inhibitor to have potency. Protease inhibitors are very efficacious in lowering the viral load to undetectable levels. A number of compounds from Boehringer-Ingelheim, InterMune/Roche, and Merck are in phase I; Medivir/Tibotec in phase II; Schering-Plough and Vertex are in phase III clinical trials.[8,9]

In early stage clinical trials, the NS3-4A inhibitor **2**, dramatically lowered plasma levels of HCV RNA when given as a single agent, although there was evidence of viral break through with selection of resistant viral variants.[11] When given in combination with PEG-IFN-α, or PEG-IFN-α and ribavirin, the selection of viral variants was minimized.[12,13] Compound **2** was well tolerated in these short viral kinetic studies and in the follow-on clinical trials. Presently, compound **2** is being tested in many late stage clinical trials in treatment naïve as well as PEG-IFN-α/ribavirin treatment-failure patients.

Compound **2** is a peptidomimetic inhibitor, whose structure is shown in Figure 1. The chiral center next to the α-ketoamide (P1) in **2** (*S*-configuration) is stable at acidic pH but is prone to epimerization through proton exchange with solvent water at alkaline pH via an enol tautomer as depicted in Figure 1. The resulting P_1-(*R*)-diastereoisomer, **3** (VRT-394; Figure 1), has shown approximately 30-fold lower inhibitory activity ($K_i > 1\,\mu M$).[10] Epimer **3** is one of the primary metabolites of **2** in vivo (the concentrations of **3** can reach up to 40% of the concentration of **2** at some time points). Because of the significant observed concentrations of **3**, understanding of the kinetics for the interconversion of **2** to **3** (in vitro and in vivo) is important to the characterization of **2**.

In an effort to increase in vivo exposure of the biologically active drug **2**, we substituted the P_1-proton with a deuterium and examined the net effect on in vitro stability and in vivo exposure in rats. This strategy of specific deuteration, which has long been in use in the investigation of organic and enzymatic reaction mechanisms and biosynthetic pathways analysis,[17−20] was viewed as the least structurally disruptive because of the SAR sensitivity to substitution at the α-keto amide position. Isotopic substitution can result in a substantial reduction of the reaction rate (or metabolism) if the covalent bond with the substituted atom is partially broken in the rate-limiting transition state.[21,22] This primary kinetic isotope effect, which is expressed as the fold

*To whom correspondence should be addressed. Phone: 1-617-444-6616. Fax: 1-617-444-7822. E-mail: youssef_bennani@vrtx.com.

[a]Abbreviations: HCV, hepatitis C virus; AUC, area under curve; PEG-IFN-α, pegylated interferon alpha; STAT-C compounds, specifically targeted antiviral therapies for hepatitis C; NIs, nucleoside inhibitors; NNIs, non-nucleoside inhibitors; RNA, ribonucleic acid; IV, intravenous; PO, oral administration.

Published on Web 11/06/2009

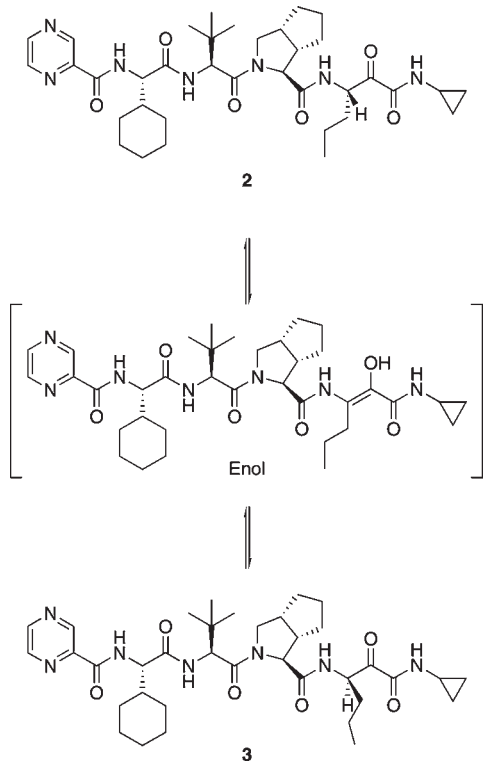

Figure 1. Reaction scheme for **2** and its (*R*)-epimer (**3**) interconversion.

decrease in rate constant for the deuterium substitution, k_H/k_D, can be as high as 7−10-fold. Kinetic isotope effect studies have long been employed to identify metabolic fate of drug substances, to determine rate-limiting steps of organic and enzymatic reactions, and to infer the rate-limiting transition-state structures.[23]

In this study, it was investigated whether the in vitro rate of epimerization of **1** (d-telaprevir) was slower than that of **2** in rat, dog, and human plasma and whether higher *S*-diastereoisomer/*R*-diasteroisomer ratios could be obtained in rat plasma after administration of **1** as compared to administration of **2**.

Herein we report the synthesis of **1**, its kinetic stability compared to **2** as a function of buffer pH, plasma stability, and pharmacokinetic profiles in rats after intravenous and oral administration.

Synthesis of 1. The synthesis of **1**, described in Scheme 1, started with 2-hexyne-1-ol **4**, which was reduced with Red-Al, and the subsequent intermediate was quenched with D_2O to deliver 3-deutero-allylic alcohol **5** in high isotope content (99%) and high reaction yield (83%). Oxidation of the alcohol **5** with MnO_2 to the corresponding aldehyde **6** was achieved in excellent yield (90%). Compound **6** was further oxidized to the carboxylic acid **7** using standard methods. At this stage, the deuterium incorporation was not determined because of nonionization. Amide formation of compound **8** with cyclopropylamine proceeded in 65% yield using isobutyl chloroformate in the presence of *N*-methyl morpholine. The mass spectral analysis showed the preservation of the deuterium content at 99%. Epoxidation of **8** was achieved with urea hydrogen peroxide in trifluoroacetic anhydride to yield **9**. The crude reaction mixture from above was used in the next step without further purification. Epoxide **9** was regiospecifically ring-opened with sodium azide to intermediate **10**, the reduction of which, in the presence of palladium on carbon, gave the racemic mixture of α-hydroxy-β-amino amide **11** in good overall yield (70%). At this stage, the mass spectral analysis revealed the deuterium content to be unchanged (∼99%). Chiral resolution of amide **11** with deoxycholic acid, followed by hydrolysis with hydrochloric acid, afforded enantiomerically pure key intermediate **13** in high deuterium content (∼99%), as assessed by chiral HPLC and mass spectroscopy, respectively. Amine **13**, the synthesis of which was reported earlier for **2**,[24] underwent amide-coupling with carboxylic acid **14**[24] to give the alcohol **15**. Tempo oxidation of **15** gave the desired final compound, **1**. The combined yield for the amide coupling and oxidation steps was 80%. The mass spectral analysis confirmed the deuterium content of the final product, **1**, at 97%. Experimental details of the synthesis of **1** are given in the Materials and Methods section.

In Vitro Characterization of 1. The antiviral characteristics of **1** and **2** were assessed side-by-side in biochemical assays. In the enzyme inhibition assay with full-length NS3-4A protease, **1** had a K_i value of 20 nM, which is similar to the value of 44 nM for **2**.[10] In the viral replication assay (replicon assay) **1** and **2** had IC_{99} values of 4.0 and 3.3 μM, respectively. Therefore, the in vitro antiviral properties of **2** are not significantly altered upon substitution with deuterium in **1**.

Compounds **1** and **2** were also subjected to buffer stability studies in solutions of varying pH from 1 to 9. Aliquots were withdrawn as a function of time and analyzed by LC-MS for the content of **1**, **2**, and the biologically inactive diastereoisomer **3**. The LC-MS analysis is described in the General Experimental Details. Below pH 7, the epimerization rate was insignificant over a 3 day period (data not shown). The percentage of **3** formed at pHs 7 and 9 were plotted as a function of time in Figure 2. These data were fitted to eq 2, where B and B_{eq} are % of **3** at time t and t_∞, respectively, and k_{obs} (the sum of rate constants for the forward and reverse reactions as shown in eq 1) is the rate constant for the approach to equilibrium. The k_{obs} for **2** was not dependent on the phosphate concentration at pH 7 (Table 1) and the epimerization half-life at pH 7 was ∼35 h. The rate-constant for epimerization of **2** at pH 9 was 19-fold higher than that at pH 7 indicating that specific base-catalyzed (HO^-) component of epimerization reaction dominated at alkaline pH. The equilibrium concentration of **3**, B_{eq}, was determined to be between 35 and 40% of the total amount of **2** and **3**.

At pH 7 and 9, compound **1** was more stable than **2**, and the observed kinetic isotope effect on the initial rate of **3** formation was approximately 5-fold. Deuterium substitution, therefore, significantly suppresses the inactivation of **2** via epimerization. Kinetic isotope effects of such magnitude for the substitution of hydrogen with deuterium have been observed previously in a number of reactions where a C−H bond was being modified.[18]

$$\mathbf{2} \underset{k_r}{\overset{k_f}{\rightleftharpoons}} \mathbf{3} \quad (1)$$

$$B = B_{eq}(1 - e^{(-k_{obs})t}) \quad (2)$$

The stability of **1** and **2** was also tested in plasma at 1 and 10 μM concentrations. Because the stability profile was similar for 1 and 10 μM concentrations, only 1 μM data is shown in Figure 3. The relative initial rates and the associated kinetic isotope effects are presented in Table 2. It is

Scheme 1. Synthesis of **1**

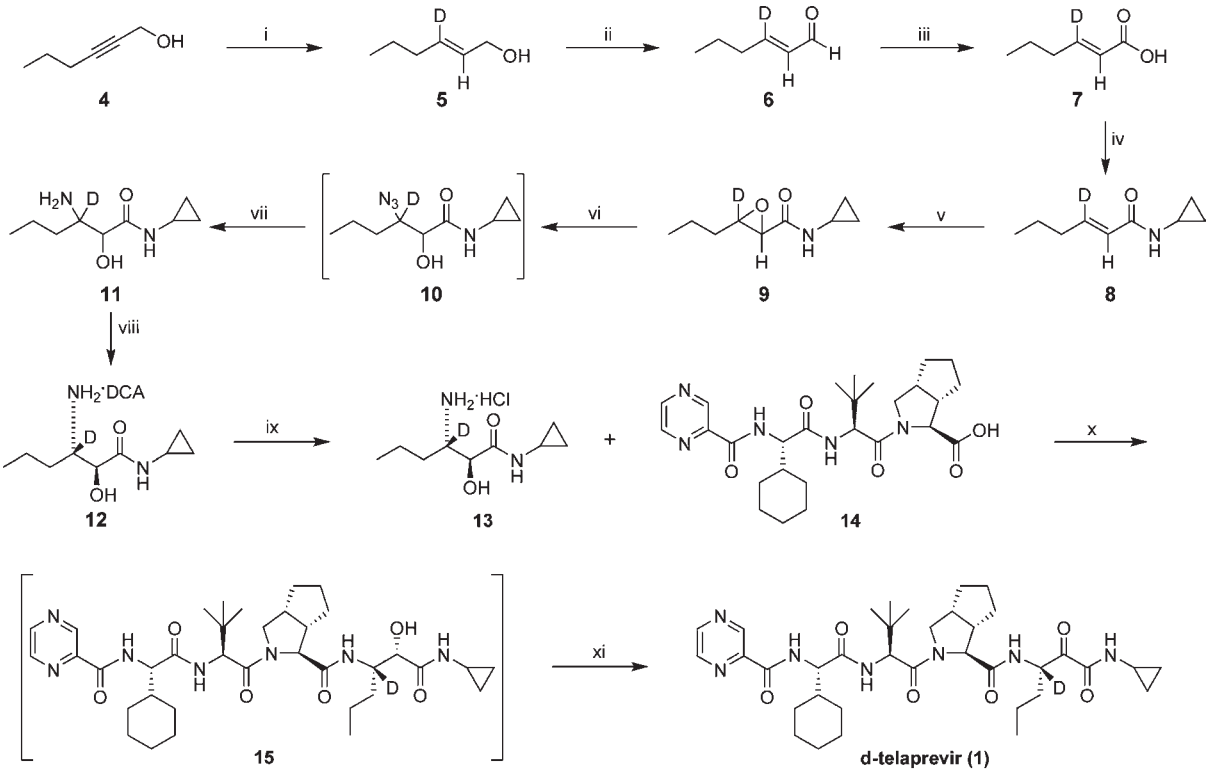

i) 1. Red-Al; 2. D_2O (95% 2 steps), ii) MnO_2 (90%), iii) $NaClO_2$, NaH_2PO_4, 2-methyl-2-butene, *t*-BuOH (75%), iv) c-Propyl amine, isobutyl chloroformate, NMM, CH_2Cl_2 (65%), v) Urea hydrogen peroxide, TFAA, *p*-TsOH, CH_2Cl_2 (86%), vi) NaN_3, $MgSO_4$, MeOH, vii) H_2 (3 atm) Pd/C, 25C, 5 hrs (70% 2 steps), viii) Deoxycholic acid, THF (40%), ix) HCl, 2-propanol (75%), x) **11**, EDC, HOBt, CH_2Cl_2, xi) Tempo, NaOCl, $NaHCO_3$, CH_2Cl_2, H_2O (80% 2 steps).

obvious that human plasma catalyzed the epimerization by a factor of about 10 compared to buffer (used as a control), while the rat or dog plasma showed less effect on the epimerization rates (Table 2). The concentration of **3** reached a steady state level of approximately 40% of the concentration of the initial **2** in human plasma, which is similar to what was observed in phosphate buffer. The compound **1** was more stable in all plasma samples when compared to **2**. The kinetic isotope effect on the initial rate of epimerization was in the range of 4−7 for dog, rat, or human plasma-catalyzed samples. The k_{obs} value for the approach to equilibrium in human plasma-catalyzed epimerization of **2**, obtained by fitting the progress curve data to eq 2, was 0.038 min^{-1} yielding a half-life of ~20 min. This has the effect of reducing the concentration of **2** by 35% (by conversion to **3**) over the course of approximately an hour. In that period only 10% of the deuterated drug was converted to **3** by epimerization (Figure 3). Epimerization of **1** also results in the production of **3** because the abstracted deuterium will be exchanged with a proton in the solvent water. Compounds **1** and **2** go through the same enol tautomeric intermediate (Figure 1 and eq 3), therefore, they have the same probability to generate **3** versus **2**, depending on which side of the enol intermediate receives the proton. We followed the kinetics of the appearance of **3** as well as the formation of **2** from **1**.

As is clear from the data for compound **1** (Figure 4), the overall production of **2** is 1.4-fold faster than the formation of the inactive epimer **3**. Therefore, the rate constant leading to the formation of **2** (k_v) is 1.4-fold larger than that leading to the formation of the inactive epimer (k_e). This observation is in line with previous work, indicating that the equilibrium favors **2** over **3** by a 60:40 ratio.

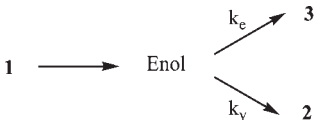

(3)

In all in vitro conditions studied, **1** was significantly more stable than **2** with respect to epimerization to form **3**. The next challenge was to determine if the additional in vitro stability of **1** would translate to increased exposure in vivo. As a first approximation, both **1** and **2** should have similar chemical and metabolic reactivity at all other sites on the molecule except for the isotopic center. Therefore, the advantage bestowed by the isotopic substitution depends on what the elimination mechanisms are with respect to epimerization. Short of testing its metabolic stability in man, the pharmacokinetics of **1** in rats was obtained.

In Vivo Characterization. Both **1** and **2** were administered to rats at 1 mg/kg IV and 10 mg/kg PO. In all experiments the concentrations of the active drug (**1** and **2**) and **3** in plasma were monitored as a function of time.

When **1** and **2** were dosed IV separately, the PK profiles were virtually identical (Figure 5A). However, when **1** and **2** were dosed PO, significant differences were observed in the PK profile (Figure 5B): (a) higher levels of **1** were observed at several time points, (b) **2** was observed over time, albeit at a low level (< 4%), in **1** administered rats, and (c) **3** levels were

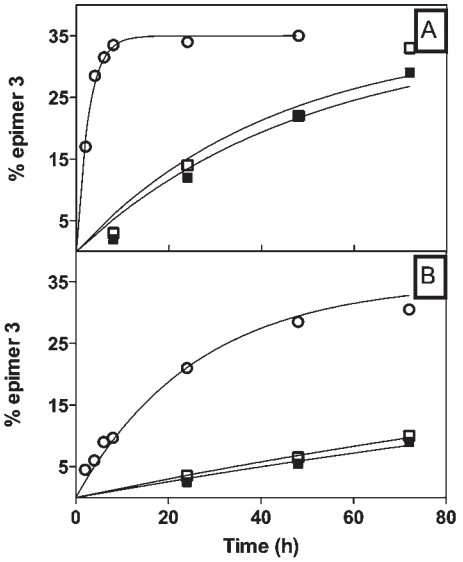

Figure 2. Epimerization rate for **2** (A) and **1** (B) in buffer. The initial concentration of **2** and **1** were 0.25 mg/mL in all experiments (□: pH 7 water; ■: pH 7 phosphate buffer (0.05 M); ○: pH 9 borate buffer (0.1 M)). Aliquots were drawn at various intervals, processed, and analyzed for the content of **3**, **2**, and **1**, as described in General Experimental Details.

Table 1. Epimerization Rate Constants for **2**

medium	k_{obs} (hr^{-1})[a]	rel. rate
pH 7 (H_2O)	0.020 ± 0.002	1
pH 7 (0.05 M phosphate)	0.023 ± 0.004	1
pH 9 (0.1 M borate)	0.375 ± 0.019	19

[a] k_{obs} is the sum of forward (k_f) and reverse (k_r) rate constants for the epimerization of **2**, as given in eq 1.

Table 2. Effect of Plasma on the Epimerization of **2** and **1**

		kinetic isotope effect[b] (k_H/k_D)	
medium	relative rate[a]	@ 1 μM	@ 10 μM
buffer (pH 7.4)	1	5	6
rat plasma	1.0 − 1.5	7	7
dog plasma	1.4 − 3.4	4	6
human plasma	> 8	> 5	> 5

[a] Initial rate of epimerization of **2**. [b] Standard error of ±1.

less in **1** dosed animals. These observations are qualitatively in agreement with the expected effect of deuterium in **1**. Each time point represents an average concentration observed in three rats. Because the animal-to-animal variability was high, it was not possible to confidently conclude if the AUC increase for **1** was statistically significant. To this end, the PO studies were repeated with a 50:50 mixture of **1** and **2** and the number of rats in the study were increased to six. By formulating the mixture of **1** and **2**, any animal-to-animal variability is removed because each animal is exposed to both **1** and **2** at the same time. Instead of plotting the absolute concentration of **1** and **2** in the PO samples, we plotted the mean ratio of **1** over **2**, as shown in Figure 6, as this gives a direct estimate of any increase in **1** due to its increased stability. The actual concentrations of **1** and **2** are presented as supplement data. The peak concentration of the active drug (**1** or **2**) was about 200 ng/mL. A cutoff of < 10 ng/mL was used to exclude data points that may be unreliable.

As the isotopic content of **1** is 97%, the 50:50 mixture sample will produce a ratio of **1** over **2** of 0.94, as indicated by the dashed line in Figure 6. It is obvious from the PO data in

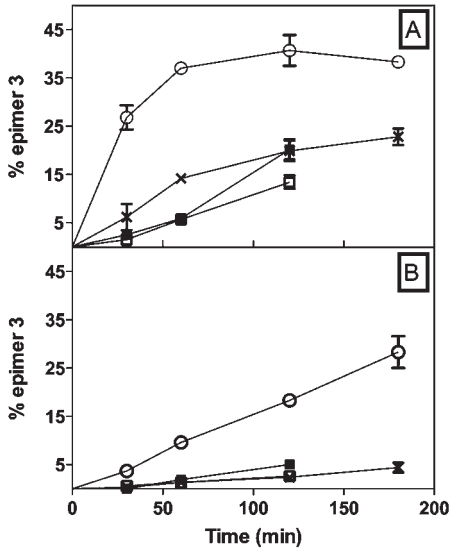

Figure 3. Stability of **2** (panel A) and **1** (panel B) in plasma samples. Compound **2** or **1** dissolved in DMSO was added either to pH 7.4 buffer (0.1 M phosphate; ×), rat plasma (□), dog plasma (■), or human plasma (○) to a final concentration of 1 μM and 10 μM (data not shown). The final DMSO concentration was 1%. Aliquots withdrawn at various intervals were processed and analyzed as in General Experimental Details.

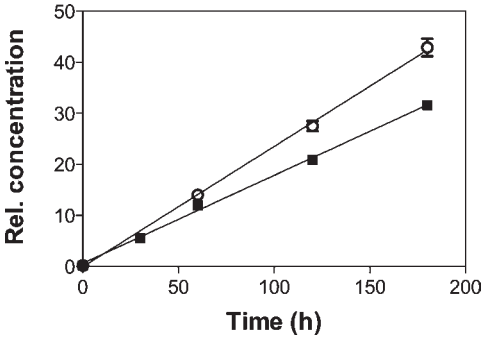

Figure 4. Appearance of **3** and **2** from **1** in human plasma. The DMSO solution of **1** was added to human plasma to a final concentration of 10 μM. Aliquots were drawn at various intervals, processed, and analyzed for the content of **2** (○) and **3** (■) as in General Experimental Details.

Figure 6 that most of the time points are above this reference line. The ratio peaks at about 2 to 3 h after dosing to a net increase of 12−15%. This is consistent with the observations in Figure 5B. Interestingly, a similar effect was not observed in the IV-dosed animals (Figure 5A); the lack of a significant difference may be due to variability in the data. The increase in the AUC for PO-dosed **1** is still small (13%), but observable. This analysis ignores the fact that a small portion of **2** was indeed generated from **1**, putting 13% increase in the AUC as a lower limit. Because the epimerization half-life is long (> 4 h) in rat plasma compared to the terminal half-life (~1.5 h; Figure 5B) in vivo, the observed small increase in the AUC for **1** is expected.

Summary

It has been well documented in the literature that isotopic substitution can alter physical properties of a compound.[17−25] However, the property changes will be subtle for atomic substitution compared to appending a chemical group.

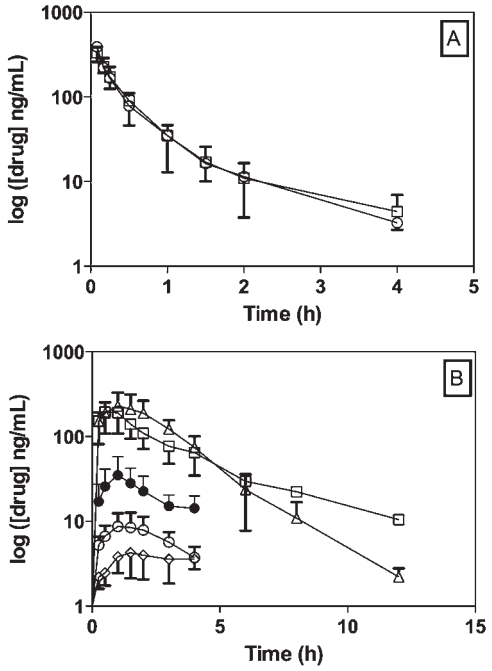

Figure 5. IV and PO dose−response curves for **2** and **1** dosed separately in rats. (A) **2** or **1** was given at 1 mg/kg dose to rat by injection into a preimplanted jugular cannula. Blood was withdrawn at specified intervals, the drug substance was extracted as in Materials and Methods and analyzed by LC/MS. The (□) and (○) represent **2** and **1** concentrations, respectively. (B) **1** and **2** were given at 10 mg/kg dose to rat by gavage, blood samples withdrawn at specified times, extracted as in Materials and Methods, and analyzed by LC/MS. The (□) and (△) represent the parent drug from **2** and **1**, respectively. The (●) and (◇) represent **3**, the metabolite from **2** and **1**, respectively. The (○) represents **2** formed from **1**.

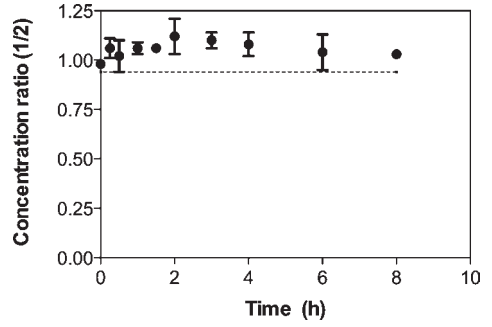

Figure 6. PO dosing of 50:50 mixture of **1** and **2**. A 50:50 mixture of **1** (97% isotopic purity) and **2** was formulated as given in the General Experimental Details and orally administered at 10 mg/kg to six male Sprague−Dawley rats. Blood samples were collected at specified times, extracted, and analyzed by MS. The ratio of **1** to **2** is plotted as a function of time. The dashed line corresponds to the initial ratio of **1** to **2** of 0.94. The actual concentrations of **2** are provided in Table 1 of the Supporting Information.

Therefore, isotopic substitution is an attractive way to boost the concentration of the active drug by slowing down either the oxidative metabolism or the epimerization rate, as exemplified in the case of **2**, without significantly altering the pharmacological properties of the drug. Currently we do not know of any deuterated drug on the market. However, a number of approved drugs were deuterated either with the intention to improve their stability or to understand the metabolic fate.[18] Recently, one publication reported that oral administration of deutero-rofecoxib in rats[26] resulted in 1.53- and 1.60-fold increases in the AUC and C_{max}, respectively. Other examples of deuterated drugs exhibiting superior properties over their counterparts in preclinical studies include 3′-d_2-butethal, showing over a 2-fold increase in sleep time[27] in mice, and deuterated sildenafil, with higher selectivity for phosphodiesterases.[28] Herein, we showed that specific deuteration of **2** led to increased pH and plasma stability in vitro. In rats, **1** exhibited a small but measurable increase in AUC and the clearance of **2** is not dominated by epimerization to **3**. Based on the epimerization of **1** to **3** in vitro, it is possible that the AUC in humans will be more significantly impacted than the minimal effect observed in rats, however, to determine this it would be necessary to dose **1** in human subjects.

Materials and Methods

General Experimental Details. All commercial reagents and anhydrous solvents were obtained from commercial sources and were used without further purification, unless otherwise specified. Mass samples were analyzed on a Micro Mass ZQ, ZMD, Quattro LC, or Quatro II mass spectrometer operated in a single MS mode with electrospray ionization. Samples were introduced into the mass spectrometer using flow injection (FIA) or chromatography. The mobile phase for all mass analysis consisted of acetonitrile−water mixtures with either 0.2% formic acid or ammonium formate. The high-resolution mass spectrum was measured using a 9.4T APEX III FTMS Bruker Daltonics instrument. The following HPLC methods were used to obtain the reported retention times. (i) Method A: YMC ProC18 column, 2.0 × 50 mm; linear gradient from 5 to 95% CH_3CN in H_2O over 15 min (0.1% trifluoroacetic acid); flow rate 1 mL/min; 214/254 nM. (ii) Method B: Daicel Chiralpak AD-H, 4.6 × 50 mm; isocratic gradient 92% heptane, 8% ethanol for 40 min (0.1% methanesulfonic acid); flow rate 1.0 mL/min at 5 °C; detection diode array. (iii) Method C: YMC-Pack PVA-Sil NP, 4.6 × 50 mm; linear gradient from 2 to 90% heptane in THF over 45 min (0.1% AcOH, 0.001% TFA); flow rate 1.5 mL/min; detection diode array. ^{1}H NMR spectra (δ, ppm) was recorded either using a Bruker DRX-500 (500 MHz) or a Bruker Avance II-300 (300 MHz) instrument. Column chromatography was performed using Merck silica gel 60 (0.040−0.063 mm). The purity of all intermediates and final product showed a purity of ≥95%, determined by HPLC and HRMS.

(*E*)-Hex-3-deutero-2-en-1-ol (5). To a three-neck 250 mL round-bottom flask equipped with mechanical stirrer and reflux condenser was charged 2-hexyn-1-ol **4** (10 g, 0.1 mol) and THF (100 mL, 10 vol). The resulting mixture was cooled down to 0 ± 5 °C and then Red-Al (65% in toluene, 32 mL, 1.6 equiv) was added slowly under a nitrogen atmosphere between 0 and 20 °C. The resulting mixture was allowed to warm up to 25 °C and stirred for 5 h. The reaction mixture was cooled down to −5 ± 5 °C, and D_2O (8.2 g, 4 equiv) was added dropwise between 0 and 15 °C. To the resulting mixture was charged isopropyl acetate (50 mL, 5 vol) and saturated NH_4Cl solution (50 mL, 5 vol). After stirring the mixture for 10 min, the white solid formed was filtered out. The organic layer from the filtrate was separated and the aqueous layer was extracted with isopropyl acetate (30 mL, 3 vol). The organic layers were combined and washed with water (30 mL, 3 vol), dried over $MgSO_4$, and concentrated to afford compound **5** (9.8 g, 95%) as a colorless oil. The crude product was used for the next step without further purification. HPLC (Method A) t_R = 9.128 min. For the compound: ^{1}H NMR (500 MHz, $CDCl_3$) δ 5.66 (t, 1H, J = 5.0 Hz), 4.12 (d, 2H, J = 5.0 Hz), 2.04 (t, 2H, J = 5.0 Hz), 1.38−1.46 (m, 2H), 0.93 (t, 3H, J = 5.0 Hz); ^{13}C NMR (125 MHz, CDCl3) δ 132.95 (t, J = 23.8 Hz), 128.90, 63.76, 34.17,

22.25, and 13.66. Deuterium content by LCMS/MS = 99%. HRMS = no signal in positive or negative ion modes.

(*E*)-Hex-3-deutero-2-enal (6). To a three-neck 250 mL round-bottom flask equipped with mechanical stirrer containing the alcohol **5** (10 g, 0.1 mol) in CH_2Cl_2 (150 mL, 15 vol) was charged activated MnO_2 (87 g, 10 equiv) at room temperature. After vigorous stirring for 1 h, another portion of MnO_2 (16 g, 2 equiv) was added and the shaking was continued for 4 h. The reaction solution was filtered through a pad of Celite. The solvent was removed in vacuo (25 °C, 100 mmHg) to give the crude aldehyde **6** as a pale yellowish oil (8.8 g, 90%). The crude product was used for the next step without further purification. HPLC (Method A) t_R = 10.141 min. For the compound: ^{1}H NMR (500 MHz, $CDCl_3$) δ 9.54 (d, 1H, J = 10.0 Hz), 6.14 (s, 1H), 2.34 (m, 2H), 1.55−1.60 (m, 2H), 1.00 (t, 3H, J = 5.0 Hz); ^{13}C NMR (125 MHz, CDCl3) δ 194.06, 158.32 (t, J = 23.8 Hz), 133.00, 34.53, 21.07, and 13.59. Deuterium content by LCMS/MS = no ionization. HRMS = no signal in positive or negative ion modes.

(*E*)-Hex-3-deutero-2-enoic acid (7). To a three-neck 500 mL round-bottom flask equipped with mechanical stirrer and reflux condenser was charged the aldehyde **6** (10 g, 0.1 mol), *tert*-BuOH (90 mL, 9 vol), and 2-methyl-2-butene (30 mL, 3 vol). The resulting solution was added with freshly prepared aqueous $NaClO_2$ (27.4 g, 3 equiv) and NaH_2PO_4 (62.9 g, 4 equiv) in water (200 mL) over 30 min. The reaction mixture was stirred at room temperature for 2 h. The reaction solution was cooled down to 0 °C and was added with saturated Na_2SO_3 aqueous solution until the reaction became colorless. The stirring was stopped, the organic layer was separated, and the aqueous layer was extracted with EtOAc (3 vol × 3). The organic layers were combined and concentrated in vacuo until the total volume became 3 vol. The resulting solution was extracted with 1 N NaOH (3 vol × 3), and the remaining organic layer was discarded. The combined aqueous solution was acidified with 6 N HCl to the pH 1.0. The solution was extracted with CH_2Cl_2 (3 vol × 5). The combined organic layer were dried over $MgSO_4$ and concentrated to give the acid **7** (8.7 g, 75%) as a white solid. HPLC (Method A) t_R = 9.02 min. For the compound: ^{1}H NMR (500 MHz, $CDCl_3$) δ 5.84 (s, 1H), 2.23 (t, 2H, J = 5.0 Hz), 1.51−1.55 (m, 2H), 0.98 (t, 3H, J = 5.0 Hz); ^{13}C NMR (125 MHz, CDCl3) δ 172.33, 151.90 (t, J = 23.8 Hz), 120.71, 34.17, 21.12, and 13.63. HRMS calcd for $C_6H_9DO_2$, 116.08163; found, 116.08163. Deuterium content by LCMS/MS = no ionization.

(*E*)-*N*-Cyclopropylhex-3-deutero-2-enamide (8). A three-neck 250 mL round-bottom flask equipped with mechanical stirrer and reflux condenser was charged with the acid **7** (10 g, 0.09 mol) and isobutyl chloroformate (13 g, 1.1 equiv) in CH_2Cl_2 (100 mL, 10 vol). The resulting solution was cooled down to 0 °C, and *N*-methyl morpholine (13.2 g, 1.5 equiv) was added slowly while controlling the temperature between 0 and 20 °C. Then, the mixture was allowed to warm up to room temperature and stirred for 1 h. To the resulting solution was added cyclopropyl amine (5.9 g, 1.2 equiv), and the solution was stirred for 2 h. The reaction mixture was washed with 1 N NaOH (3 vol × 2), 1 N HCl (3 vol × 2), brine solution (3 vol), and water (3 vol). The organic layer was dried over $MgSO_4$ and concentrated to afford the crude product as an oil. The crude product was dissolved with heptane (5 vol) and cooled down to −78 °C with stirring. The precipitated solid was filtered and dried to give the amide **8** (8.7 g, 65%) as a white solid. HPLC (Method A) t_R = 8.51 min. For the compound: ^{1}H NMR (500 MHz, DMSO) δ 7.92 (s, 1H), 5.78 (s, 1H), 2.66−2.68 (m, 1H), 2.08 (t, 2H, J = 5.0 Hz), 1.38−1.42 (m, 2H), 0.87 (t, 3H, J = 5.0 Hz), 0.63 (t, 2H, J = 3.0 Hz), 0.40 (t, 2H, J = 3.0 Hz); ^{13}C NMR (125 MHz, $CDCl_3$) δ 165.88, 141.52 (t, J = 23.8 Hz), 124.25, 33.02, 22.15, 20.09, 13.44, and 5.65. HRMS calcd for $C_9H_{15}DNO$, 155.12892; found, 155.12873. Deuterium content by LCMS/MS = 99%.

3-Deutero-*N*-cyclopropyl-3-propyloxirane-2-carboxamide (9). To a three-neck 250 mL round-bottom flask equipped with mechanical stirrer and containing the amide **8** (10 g, 0.06 mol), urea hydrogen peroxide (25 g, 4 equiv), and *p*-TsOH (12.3 g, 1 equiv) in CH_2Cl_2 (100 mL, 10 vol) at 0 °C was added trifluoroacetic anhydride (40.9 g, 3 equiv) in CH_2Cl_2 (50 mL, 5 vol) over 30 min. The reaction mixture was heated to 40 ± 5 °C and stirred for 3 h. After cooling down the reaction solution to 0 °C, the reaction was quenched by adding 6 N NaOH (100 mL, 10 vol) slowly and stirring for 30 min. The organic layer was separated, and the organic layer was washed with brine (5 vol) and water (5 vol). The resulting organic layer was dried over $MgSO_4$ and evaporated to give the epoxide **9** (9.7 g, 86%) as pale yellow oil. The crude product was used for the next step without further purification. HPLC (Method A) t_R = 7.86 min. For the compound: ^{1}H NMR (500 MHz, DMSO) δ 8.01 (s, 1H), 3.09 (s, 1H), 2.63−2.65 (m, 1H), 1.39−1.54 (m, 4H), 0.91 (t, 3H, J = 5.0 Hz), 0.60 (t, 2H, J = 3.0 Hz), 0.45 (t, 2H, J = 3.0 Hz); ^{13}C NMR (125 MHz, $CDCl_3$) δ 168.67, 56.73 (t, J = 26.3 Hz), 54.08, 32.69, 22.06, 18.59, 13.56, 5.38, and 5.37. HRMS calcd for $C_6H_{15}DNO_2$, 171.12383; found, 171.12383. Deuterium content by LCMS/MS = no ionization.

3-Azido-3-deutero-*N*-cyclopropyl-2-hydroxyhexanamide (10). To a three-necked 250 mL round-bottom flask equipped with mechanical stirrer and reflux condenser containing the epoxide **9** (10 g, 0.06 mol) and anhydrous magnesium sulfate (14.1 g, 2.0 equiv) in MeOH (100 mL, 10 vol) was added sodium azide (15.3 g, 4.0 equiv) in one portion. The resulting mixture was heated to 65 ± 5 °C and stirred for 5 h. The reaction solution was cooled down to room temperature and isopropyl acetate (100 mL, 10 vol) was added and stirred for 10 min. The mixture was filtered through a pad of Celite to get rid of insoluble salts and the resulting clear solution was concentrated to 3 vol. To the resulting solution was added isopropyl acetate (170 mL, 17 vol) and the mixture was stirred for 10 min. Again, the solution was filtered through a pad of Celite to afford the product **10** as a clear solution in isopropyl acetate (about 200 mL) for the next step without further purification. HPLC (Method A) t_R = 8.88 min. For the compound: ^{1}H NMR (500 MHz, DMSO) δ 7.91 (s, 1H), 6.00 (d, 1H, J = 5.0 Hz), 4.03 (d, 1H, J = 5.0 Hz), 2.66−2.67 (m, 1H), 1.30−1.58 (m, 4H), 0.88 (t, 3H, J = 5.0 Hz), 0.60 (t, 2H, J = 3.0 Hz), 0.48 (t, 2H, J = 3.0 Hz); ^{13}C NMR (125 MHz, CDCl3) δ 171.93, 73.43, 62.90 (t, J = 23.8 Hz), 29.25, 22.11, 18.89, 13.55, and 5.42. HRMS calcd for $C_9H_{16}DN_4O_2$, 214.14088; found, 214.14076. Deuterium content by LCMS/MS = 99%.

3-Amino-3-deutero-*N*-cyclopropyl-2-hydroxyhexanamide (11). A 500 mL autoclave hydrogenation reactor equipped with mechanical stirrer containing the azido compound **10** (200 mL, 0.05 mol) in isopropyl acetate (obtained in the previous step) was charged with Pd/C (10% Pd, water 50%, 0.8 g). The solution was charged with nitrogen (1.0 atm) and released three times and then charged with hydrogen (3.0 atm) and released three times. The resulting solution was charged with hydrogen (3 atm) and stirred for 5 h. After releasing the hydrogen gas, the solution was purged with nitrogen for 5 min. To the resulting solution was added MeOH (30 mL, 3 vol), and the reaction mixture was heated to 50 ± 5 °C. The reaction mixture was filtered through a pad of Celite to afford a clear solution. The product was isolated by concentrating the solution at 20 ± 5 °C until 3 vol of the solution remained. The solid was collected by filtration, washed (isopropyl acetate, 3 vol), and dried to give the amine **11** (7.7 g, 70%, two steps) as a white crystalline solid. HPLC (Method A) t_R = 4.51 min. For the compound: ^{1}H NMR (500 MHz, DMSO) δ 7.70 (s, 1H), 5.31 (s, 2H), 3.68 (s, 1H), 2.64−2.66 (m, 1H), 1.10−1.50 (m, 4H), 0.82 (t, 3H, J = 5.0 Hz), 0.59 (t, 3H, J = 3.0 Hz), 0.45 (t, 3H, J = 3.0 Hz); ^{13}C NMR (125 MHz, $CDCl_3$) δ 173.61, 75.38, 52.93 (t, J = 20.0 Hz), 33.40, 21.93, 18.78, 14.01, 5.49, and 5.47. HRMS calcd for $C_9H_{18}DN_2O_2$, 188.15038; found, 188.15028. Deuterium content by LCMS/MS = 99%.

(2*S*,3*S*)-3-Amino-3-deutero-*N*-cyclopropyl-2-hydroxyhexanamide Deoxycholic Acid Salt (12). To a three-neck 250 mL round-bottom flask equipped with mechanical stirrer and containing the racemic amine **11** (10 g, 0.05 mol) in THF

(100 mL, 10 vol) was charged deoxycholic acid (15.7 g, 0.75 equiv). The reaction mixture was heated to 65 ± 5 °C and stirred for 1 h at this temperature. The resulting homogeneous mixture was cooled down to 23 ± 2 °C over 1 h, and was maintained at the same temperature range for 1 h. The precipitated solids were collected by filtration, washed with THF (50 mL, 5 vol), and dried to give the resolved amine **12** (12.4 g, 41%, enantiomeric ratio (ER) = 2:98) as a white solid. HPLC (Method B) t_R = 27.11 min. HRMS calcd for $C_9H_{18}DN_2O_2$, 188.15038; found, 188.15060. Deuterium content by LCMS/MS = 98%.

(2*S*,3*S*)-3-Amino-3-deutero-*N*-cyclopropyl-2-hydroxyhexanamide Hydrochloric Acid Salt (13). To a three-neck 250 mL round-bottom flask equipped with mechanical stirrer was charged with compound **12** and 2-propanol (62 mL, 5 vol). The solution was heated to 75 ± 5 °C and 5−6 N HCl solution in 2-propanol (12 mL, 3 equiv) was added slowly with vigorous stirring. The resulting solution was stirred at the same temperature for 1 h and was cooled down to 23 ± 2 °C. The reaction mixture was maintained at the same temperature for 1 h. The precipitated solids were collected by filtration, washed with 2-propanol (36 mL, 3 vol), and dried to give the enantiomerically pure amine **13** (3.0 g, 75%, ER = 0:100) as a white solid. HPLC (Method B) t_R = 24.86 min. For the compound: ^{1}H NMR (500 MHz, DMSO) δ 8.07 (s, 1H), 7.97 (s, 3H), 6.25 (d, 1H, J = 5.0 Hz), 4.16 (d, 1H, J = 5.0 Hz), 2.67−2.70 (m, 1H), 1.33−1.46 (m, 4H), 0.84 (t, 3H, J = 5.0 Hz), 0.61 (t, 3H, J = 3.0 Hz), 0.53 (t, 3H, J = 3.0 Hz); ^{13}C NMR (125 MHz, $CDCl_3$) δ 171.70, 70.54, 52.37 (t, J = 23.8 Hz), 29.07, 22.17, 18.04, 13.69, 5.34, and 5.30. HRMS calcd for $C_9H_{18}DN_2O_2$, 188.15038; found, 188.15048. Deuterium content by LCMS/MS = 99%.

(1*S*,3a*R*,6a*S*)-*N*-((*R*)-3-Deutero-1-(cyclopropylamino)-1,2-dioxohexan-3-yl)-2-((*S*)-2-((*S*)-2-cyclohexyl-2-(pyrazine-2-carboxamido)acetamido)-3,3-dimethylbutanoyl) Octahydrocyclopenta[*c*]pyrrole-1-carboxamide, 1. CH_2Cl_2 (6 vol) was charged into a 300 mL, three-neck flask and cooled to 0−5 °C. (1*S*,3a*R*,6a*S*)-2-((*S*)-2-((*S*)-2-cyclohexyl-2-(pyrazine-2-carboxamido)acetamido)-3,3-dimethylbutanoyl)octahydrocyclopenta[*c*]pyrrole-1-carboxylic acid **14**[29] (10.0 g, 1.0 equiv), HOBt hydrate (2.85 g, 1.1 equiv), EDCI (3.53 g, 1.1 equiv), and the chiral amine **13** (4.12 g, 1.1 equiv) were charged to the same flask in that order. NMM (3.68 mL, 2.0 equiv) was added over 10 min while maintaining the reaction temperature below 5 °C. The reaction mixture was warmed up 20−25 °C over 30 min and stirred for an additional 6 h. The reaction completion of compound **15** was monitored by HPLC. The reaction mixture was washed with water (5 vol), 1 N HCl (5 vol), and 5 wt % aq $NaHCO_3$ (5 vol) to yield a solution of (1*S*,3a*R*,6a*S*)-*N*-((*R*)-3-deutero-1-(cyclopropylamino)-2-hydroxy-1-oxohexan-3-yl)-2-((*S*)-2-((*S*)-2-cyclohexyl-2-(pyrazine-2-carboxamido)acetamido)-3,3-dimethylbutanoyl) octahydrocyclopenta[*c*]-pyrrole-1-carboxamide **15** in CH_2Cl_2.

TEMPO (0.25 g, 0.06 equiv) was added to the above alcohol **15** solution in CH_2Cl_2 and stirred at 20−25 °C until all TEMPO was dissolved. To this solution a solution of $NaHCO_3$ (1.5 equiv) in water (4 vol) was added. The resulting biphasic mixture was cooled to 0−5 °C. While maintaining the reaction temperature at 0−5 °C, a 10−13 wt % NaOCl solution (20.0 g, 1.1 equiv) was added over 30 min and stirred for an additional 1 h. The layers were separated and the organic layer was washed with H_2O (5 vol), 1% Na_2SO_3 (5 vol), and H_2O (5 vol) at 0−5 °C. Glacial acetic acid (0.12 equiv) was added to the solution of **1** in CH_2Cl_2. The organic layer is reduced to 3 vol by vacuum distillation at less than 20 °C. After distillation, the solution was brought up to 40 °C. EtOAc (0.8 vol) was added, followed by the addition of **1**. The resulting mixture was stirred for 15 min at 40 °C. EtOAc (8 vol) was added to the mixture while maintaining a temperature at 40 °C. The total volume of the slurry was then reduced to 4 vol by distillation at 30−40 °C. The resulting slurry was then cooled down to 25 °C over 1 h and stirred for an additional 1 h. The slurry was filtered. The filter cake was washed with EtOAc (3 vol), dried under vacuum with nitrogen bleed at 45 °C for 10 h, and cooled down to 20−25 °C to afford **1** (9.2 g, 80%) as a white solid. HPLC (Method C) t_R = 18.0 min. For the compound: ^{1}H NMR (500 MHz, DMSO) δ 9.21 (s, 1H), 8.91 (d, 1H, J = 2.0 Hz), 8.77 (t, 1H, J = 1.0 Hz), 8.72 (d, 1H, J = 5.0 Hz), 8.51 (d, 1H, J = 9.0 Hz), 8.25 (s, 1H), 8.22 (d, 1H, J = 9.0 Hz), 4.70 (m, 1H), 4.54 (m, 1H), 4.28 (d, 1H, J = 3.5 Hz), 3.75 (*A*BX, 1H, J_{AB} = 8.0 Hz, J_{AX} = 8.0 Hz), 3.64 (A*B*X, 1H, J_{AB} = 10.5 Hz, J_{AX} = 3.0 Hz), 2.75 (m, 1H), 2.64 (m, 1H), 1.83−1.30 (m, 16H), 1.19−1.00 (m, 6H), 0.94 (s, 9H), 0.89 (t, 3H, J = 7.0 Hz), 0.66 (m, 2H), 0.58 (m, 2H); ^{13}C NMR (125 MHz, $CDCl_3$) δ 196.91, 171.74, 170.33, 169.19, 168.93, 161.99, 161.84, 147.78, 143.96, 143.37, 143.34, 64.64, 56.31, 56.23, 54.08, 47.12, 42.18, 41.21, 35.63, 34.33, 32.01, 31.70, 31.48, 28.99, 27.92, 26.28, 25.63, 25.57, 24.56, 22.39, 22.33, 18.64, 13.66, 13.41, 5.33, and 5.27. HRMS calcd for $C_{36}H_{53}DN_7O_6$, 681.41929; found, 681.41946. Deuterium content as determined by LCMS/MS was 97%.

Stability Kinetics in Buffer. Stability kinetics were performed in four different buffers from Fisher Scientific: pH 1 (potassium chloride, SB140-500), pH 3 (potassium bipthalate, SB97-500), pH 5 (potassium bipthalate, SB102-500), pH 7 (potassium phosphate monobasic, SB108-500), and pH 9 (boric acid−potassium chloride, SB114-500). Simulated gastric fluid was prepared as specified in the U.S. Pharmacopeia (USP), giving a sodium chloride concentration of 2 mg/mL, a pepsin concentration of 3.2 mg/mL, and a final pH of 1.2 adjusted by 12 N HCl. Simulated intestinal fluid was prepared as a 6.8 mg/mL monobasic potassium phosphate solution and the pH was adjusted to 6.8 by 0.2 N sodium hydroxide. Due to the low aqueous solubility of **2** and **1**, a 1:1 (v/v) mixture of aqueous buffer (above) and acetonitrile was prepared to test the stability of compounds at different pHs. The analytes were incubated at RT or 37 °C with buffers/ACN mixture at final concentrations of 0.25 mg/mL. Liquid chromatography (HPLC) was used to quantitate the concentrations of the inactive **3** and **2** or **1** in the buffer at various time points from time 0 to 3 days.

Stability Kinetics in Plasma. The analytes (**1** or **2**) were incubated at 37 °C with rat, dog, and human plasma at final concentrations of 1 or 10 μM. The concentrations of analytes in plasma were monitored at various time points over time. Specifically, 495 μL aliquots of rat, dog, and human plasma were preincubated in cluster tubes in a shaking 37 °C water bath. The 5 μL volumes of 0.1 and 1.0 mM stock solutions of **1** and **2** were added to the aliquots. The final concentrations were 1 and 10 μM of **1** and **2**. All incubations were conducted in triplicates in a shaking 37 °C water bath. Control incubations were conducted in 0.1 M KPO_4 buffer. Incubation times were 0, 30, 60, and 120 min for rat and dog, and 0, 30, 60, 120, and 180 min for buffer and human plasma. At the end of the incubation, 100 μL volumes were transferred to cluster plates placed on dry ice and flash frozen. The plates were sealed and stored in −80 °C freezer until extraction. This procedure was followed for all concentrations of **1** and **2** (1 and 10 μM) investigated using buffer and plasma samples from all species investigated.

Sample Extraction and Preparation for LC-MS Analysis. Prior to thawing the samples, 5 μL formic acid and 10 μL of internal standard solution were added to all the samples, followed by 1200 μL ethyl acetate, using a Quadra 3 multichannel pipetter (TomTec, Hamden CT). The plate was then covered tightly and vortexed for 20 min and centrifuged at 3000 rpm for 10 min. After centrifugation, 900 μL of supernantant was transferred to a V-bottomed 96 deep-well plate. The solution was then dried under nitrogen gas at flow rate of 60 L/min at 25 °C for about 30 min. The contents of the plate were then reconstituted with 100 μL of ethyl acetate. The reconstituted solution was transferred into a 96-well plate containing glass inserts. The plate was covered and 20 μL was injected into LCMS/MS.

Instrumentation

All sample analysis was carried out on an API 4000 mass spectrometer from Applied Biosystems/MDS Sciex (Applied

Biosystems, Foster City, CA) equipped with Turbo V sources and TurboIonspray interface. The HPLC system consisted of an Agilent series 1100 binary pump (Agilent Technologies, Palo Alto, CA). The auto sampler was a CTC Analytics PAL autosampler (CTC Analytics AG, Zwingen, Switzerland). All instrumentations were controlled and synchronized by Analyst software (version 1.4.1) from Applied Biosystems/MDS Sciex.

Liquid Chromatographic and Mass Spectrometric Methods. Chiral separation was accomplished on a ChiralPak AD column (Chiral Technologies, Inc., West Chester, PA). The mobile phase consisted of two solvents, solvent A (2-propanol) and solvent B (*n*-heptane). The gradient was maintained at 10% A for 0.2 min, followed by a linear increase to 50% A in 5 min, and kept at 50% B for 6 min, and then the gradient was decreased to 10% A in 0.01 min. The column was then equilibrated at 10% A for 9.99 min. The total run time for each injection was 20 min. The flow rate was 0.7 mL/min. The injection volume was 20 μL. To improve the signal, a makeup solvent consisting of 0.2% formic acid in water was added at a flow rate of 0.1 mL/min post column.

The MRM parameters were optimized by infusing the standard solutions of test compound and internal standard in the mixture of 0.1% formic acid in 50% acetonitrile with water. The MRM transitions for **2** was 680.36 > 322.30; **1** was 681.36 > 323.30; and the internal standard of isotope labeled **2** with 11 deuterium atoms was 691.36 > 322.30. The dwell time of each transition was 150 ms.

Pharmacokinetics in Rat. Male Sprague−Dawley rats (six/dose group; weight range 275−300 g) from Charles River Laboratories with preimplanted jugular and carotid cannulas were dosed with 10 mg/kg of **2** or 10 mg/kg of **1** by the oral route. The dosing vehicle contained 1 mg/mL of **1** or **2** in a vehicle made from a rotovapped solid dispersion containing 49.5% **2**, 49.5% HPMC-AS, and 1% SLS, which was dissolved in 1% HPMC-AS and 10% vitamin E TPGS. The dosing volume was 10 mL/kg.

Two additional groups of male Sprague−Dawley Rats (six/dose group; weight range 230−270 g) from Charles River Laboratories with preimplanted jugular and carotid cannulas were dosed with 1 mg/kg of **2** or 1 mg/kg of **1** by the intravenous route. The dosing vehicle contained 1 mg/mL of **1** or **2**, which was dissolved in 10% dimethyl isosorbide, 15% ethanol, 40% propylene glycol, and 35% D5W (dextrose 5% in water). The intravenous formulation was filtered using a Millex-LG filter (Millipore Corporation, Bedford, MA) and injected through the preimplanted jugular cannula.

A fifth group of six male Sprague−Dawley rats (weight range 250−275 g) from Charles River Laboratories with preimplanted jugular and carotid cannulas were dosed with 10 mg/kg of **1** and **2** in a 50/50 mixture by the oral route. The dosing vehicle contained 0.5 mg/mL of **2** and 0.5 mg/mL **1** in a vehicle made from a rotovapped solid dispersion containing 49.5% **2**, 49.5% HPMC-AS, and 1% SLS, which was dissolved in 1% HPMC-AS and 10% vitamin E TPGS. The dosing volume was 10 mL/kg.

Blood samples were collected from each rat at 0 (predose), 0.25, 0.5, 1, 1.5, 2, 4, 6, 8, 12, and 24 h after oral dosing. Blood samples (0.250 mL) were collected using the Instech Automated Blood Samples (Model ABS11, Instech Laboratories, Plymouth Meeting, PA) into EDTA containing tubes that were maintained at 4 °C. The plasma was isolated from the blood by centrifugation (Eppendorf model 5415D centrifuge, 2 min at 16100 rpm) within 30 min after sample collection. A total of 100 μL of the resulting plasma was combined with 5 μL of 10% formic acid (Fluka, Germany). The acidified plasma sample was frozen at approximately −60 °C until analysis with the LC/MS/MS.

Pharmacokinetic parameters were determined using plasma concentration−time profiles and tissue concentration−time profiles of **1** and **2** in rats at scheduled (nominal) sampling times with non compartmental pharmacokinetic methods using WinNonlin Professional Edition software, version 5.1.1 (Pharsight Corporation, Mountain View, CA).

Acknowledgment. We would like to thank Nigel Ewing and Wojciech Dworakowski for help in generating the supporting data, and Dr. Françoise Berlioz-Seux, Dr. Lindsay McNair, Dr. Valérie Philippon, and Sarah Cowherd from Vertex Pharmaceuticals for their input and editorial help in preparing this manuscript.

Supporting Information Available: Analytical data of compounds **1** and **5**−**13**. This material is available free of charge via the Internet at http://pubs.acs.org.

References

(1) (a) Memon, M. I.; Memon, M. A. Hepatitis C: An epidemiological review. *J. Virol. Hepat.* **2002**, *9*, 84–100.(b) also see: http://www.who.int/vaccine_research/diseases/viral_cancers/en/index2.html.
(2) Fried, M. W.; Shiffman, M. L.; Reddy, K. R.; Smith, C.; Marinos, G.; Goncales, F. L., Jr.; Haussinger, D.; Diago, M.; Carosi, G.; Dhumeaux, D.; Craxi, A.; Lin, A.; Hoffman, J.; Yu, J. Peginterferon α-2a plus Ribavirin for chronic hepatitis C virus infection. *N. Engl. J. Med.* **2002**, *347*, 975–982.
(3) Strader, D. B.; Wright, T.; Thomas, D. L.; Seeff, L. B. Diagnosis, management, and treatment of hepatitis C. *Hepatology* **2004**, *39*, 1147–1171.
(4) Kolykhalov, A. A.; Mihalik, A. K.; Feinstone, S. M.; Rice, C. M. Hepatitis C virus encoded enzymatic activities and conserved RNA elements in the 3′ nontranslated region are essential for virus replication in vivo. *J. Virol.* **2000**, *74*, 2046–2051.
(5) Burton, J. R., Jr.; Everson, G. T. HCV NS5B poymerase inhibitors. *Clin. Liver Dis.* **2009**, *13*, 453–465.
(6) Kronenberger, B.; Zeuzem, S. Current and future treatment options for HCV. *Ann. Hepatol.* **2009**, *8*, 103–112.
(7) Beaulieu, P. L. Recent advances in the development of NS5B polymerase inhibitors for the treatment of hepatitis C virus infection. *Expert Opin. Ther. Pat.* **2009**, *19*, 145–164.
(8) Reiser, M.; Timm, J. Serine protease inhibitors as anti-hepatitis C virus agents. *Expert Rev. Anti-Infect. Ther.* **2009**, *7*, 537–547.
(9) Chen, K. X.; Njoroge, F. G. A review of HCV protease inhibitors. *Curr. Opin. Invest. Drugs* **2009**, *10*, 821–837.
(10) Perni, R. B.; Almquist, S. J.; Byrn, R. A.; Chandorkar, G.; Chaturvedi, P. R.; Courtney, L. F.; Decker, C J.; Dinehart, K.; Gates, C. A.; Harbeson, S. L.; Heiser, A.; Kalkeri, G.; Kolaczkowski, E.; Lin, K.; Luong, Y.-P.; Rao, B. G.; Taylor, W. P.; Thomson, J. A.; Tung, R. d.; Wei, Y.; Kwong, A. D.; Lin, C. Preclinical profile of telaprevir, a potent, selective, and orally bioavailable inhibitor of hepatitis C virus NS3-4A serine protease. *Antimicrob. Agents Chemother.* **2006**, *50*, 899–909.
(11) Reesink, H. W.; Zeuzem, S.; Weegink, C. J.; Forestier, N.; Van Vliet, A.; De RooiJ, J. J. V. D. W.; McNair, L.; Purdy, S.; Kauffman, R.; Alam, J.; Jansen, P. L. M. Rapid decline of viral RNA in hepatitis C patients treated with telaprevir: A phase Ib, placebo-controlled, randomized study. *Gastroenterology* **2006**, *131*, 997–1002.
(12) Forestier, N.; Reesink, H. W.; Weegink, C. J.; et al. Antiviral activity of telaprevir and peginterferon α-2a in patients with hepatitis C. *Hepatology* **2007**, *46*, 640–648.
(13) Lawitz, E.; Rodriguez-Torres, M.; Muir, A. J.; et al. Antiviral effects and safety of telaprevir, peginterferon α-2a, and ribavirin for 28 days in hepatitis C patients. *J. Hepatol.* **2008**, *49*, 163–169.
(14) Kieffer, T. L.; Sarrazin, C.; Miller, J. S.; Welker, M. W.; Forestier, N.; Reesink, H. W.; Kwong, A. D.; Zeuzem, S. Telaprevir and

pegylated interferon-α-2a inhibit wild-type and resistant genotype 1 hepatitis C virus replication in patients. *Hepatology* **2007**, *46*, 631–639.
(15) Sarrazin, C.; Kieffer, T. L.; Bartels, D.; Hanzelka, B.; Muh, U.; Welker, M.; Wincheringer, D.; Zhou, Y.; Chu, H.-M.; Lin, C.; Weegink, C.; Reesink, H.; Zeuzem, S.; Kwong, A. D. Dynamic hepatitis C virus genotypic changes in patients treated with the protease inhibitor Telaprevir. *Gastroenterology* **2007**, *132*, 1767–1777.
(16) Poordad, F.; Shiffman, M.; Sherman, K.; Smith, J.; Yao, M.; George, S.; Adda, N.; McHutchison, J. A study of teleprevir with peginterferon α-2A (P) and ribavirin (R) in subjects with well-documented prior P/R null response, non-response or relapse: preliminary results. *J. Hepatol.* **2008**, *48*, Supplement 2, S374−S375.
(17) Melander, L.; Saunders, W. H. *Reaction Rates of Isotopic Molecules*; Wiley: New York, NY, 1980.
(18) Blake, M. I.; Crespi, H. L.; Katz, J. J. Studies with deuterated drugs. *J. Pharm. Sci.* **1975**, *64*, 367–391.
(19) Hall, L. H.; Hanslik, R. P. Kinetic deuterium isotope effects on the N-demethylation of tertiary amides by cytochrome P-450. *J. Biol. Chem.* **1990**, *265*, 12349–12355.
(20) Nelson, S. D.; Tragger, W. F. The use of deuterium isotope effects to probe the active site properties, mechanism of cytochrome P-450-catalyzed reactions, and mechanisms of metabolically dependent toxicity. *Drug Metab. Dispos.* **2003**, *31*, 1481–1498.
(21) Krauser, J. A.; Guengerich, F. P. Cytochrome P450 3A4-catalyzed testaterone 6b-hydroxylation stereochemistry, kinetic deuterium isotope effects, and rate-limiting steps. *J. Biol. Chem.* **2005**, *280*, 19496–19506.
(22) Cleland, W. W. The use of kinetic isotope effects to determine enzyme mechanism. *Arch. Biochem. Biophys.* **2005**, *433*, 2–12.
(23) Klinman, J. P. Primary kinetic isotope effects. In *Transition states of biochemical processes*; Gandour, R. D., Schowen, R. L., Eds.; Plenum Press: New York, NY, 1978.
(24) Tanoury, G. J.; Chen, M.; Jung, Y. C.; Forslund, R. E. Process for preparation of α-amino-β-hydroxycarbonyl compounds. PCT Int. Appl. WO 2007109023 A1, **2007**.
(25) Cleland, W. W.; O'Leary, M. H.; Northrop, D. B.; Eds. In *Isotope effects on enzyme-catalyzed reactions*; University Park Press: Baltimore, MD, 1977.
(26) Schneider, F.; Hillgenberg, M.; Koytchev, R.; Alken, R.-G. Enhanced plasma concentration by selective deuteration of rofecoxib in rats. *Arzneim. Forsch./Drug Res.* **2007**, *56*, 295–300.
(27) Tanabe, M.; Yasuda, D.; LeValley, S.; Mitoma, C. The pharmacologic effect of deuterium substitution on 5-*n*-butyl-5-ethylbutyric acid. *Life Sci.* **1969**, *8*, 1123–1128.
(28) Scheider, F.; Mattern-Dogru, E.; Hillgenberg, M.; Alen, R.-G. Changed phsophodiesterase selectivity and enhanced in vivo efficacy by selective deuteration of sildenafil. *Arzneim. Forsch./Drug Res.* **2007**, *57*, 293–298.
(29) Synthesis: Yip, Y.; Victor, F.; Lamar, J.; Johnson, R.; Wang, Q. M.; Glass, J. I.; Yumibe, N.; Wakulchik, M.; Munroe, J.; Chen, S.-H. P4 and P1′ optimization of bicycloproline P2 bearing tetrapeptidyl a-ketoamides as HCV protease inhibitors. *Bioorg. Med. Chem. Lett.* **2004**, *14*, 5007−5011.